яние от точки равных энергий до линии спектральных цветностей.

Значения доминантной длины волны свечения и чистоты цвета, определенные с помощью диаграммы цветности, представлены для каждого исследуемого образца в таблице 3.

На основе рассчитанных цветовых характеристик свечения исследуемых материалов можно заключить, что образцы исходного стекла и образцы содержащие Т-фазу $YNbO_4$, соактивированные ионами Tm^{3+}, очень близки по цветовым характеристикам люминесценции к коммерческим люминофорам.

Таблица 3 – Цветовые характеристики свечения образцов: λ_d – доминантная длина волны, p_e – чистота цвета

Образец	λ_d, нм	p_e
Возбуждение стоксовой люминесценции на длине волны 355 нм		
Исходное стекло	473	0.50
800°C/6 ч.	457	0.92
900°C/6 ч.	464	0.79
1000°C/6 ч.	597	0.98
Возбуждение АКЛ на длине волны 960 нм		
Исходное стекло	473	0.50
720°C/6 ч.	471	0.65

UDC 621

THERMAL LENSING PROPERTIES OF ALEXANDRITE LASER CRYSTAL

Loiko P.[1], Ghanbari S.[2], Matrosov V.[3], Yumashev K.[4], Major A.[2]

[1]ITMO University
Saint-Petersburg, Russia
[2]Department of Electrical and Computer Engineering, University of Manitoba, Canada
[3]Solix Ltd., Minsk, Belarus
[4]Center for Optical Materials and Technologies, Belarusian National Technical University
Minsk, Belarus

Alexandrite (Cr^{3+}:$BeAl_2O_4$) is a well-known crystal for tunable lasers [1–3] which have relevant applications in medicine, space LIDAR technologies, spectroscopy [4] and can replace Ti:Sapphire lasers in nonlinear microscopy. However, thermo lensing properties of alexandrite have not been studied in detail to date.

In the present paper, we aimed to measure the thermal lens in a laser alexandrite (Cr^{3+}:$BeAl_2O_4$) element under lasing conditions.

Alexandrite is orthorhombic (sp. gr. *Pnma*) and thus optically biaxial. Its optical properties are characterized in the frame of the optical indicatrix. The optical indicatrix axes are mutually orthogonal and they coincide with the crystallographic axes ***a***, ***b***, ***c***.

Thermal lensing was studied in a ***c***-cut 0.16 at. % Cr^{3+}:$BeAl_2O_4$ oriented for the ***E*** ∥ ***b*** laser polarization when placed at Brewster angle. The optical power of the thermal lens D (inverse of the focal length, $D = 1/f$) was calculated from the measured radii of the output laser mode. For this, a ray transfer matrix formalism (ABCD law) was used and the M^2 parameter of the laser beam was accounted for. The thermal lens was considered as a thin astigmatic lens located in the center of the crystal. The radii of the laser mode were measured along the horizontal (x) and vertical (y) directions using a beam profiler.

The schematic of the CW Alexandrite laser is shown in Fig. 1(a). The slab-shaped laser crystal was oriented at a Brewster angle (θ_B). Its dimensions were 3×5×7 mm^3 (height × width × length). It was mounted in an Al-holder and passively cooled from 4 sides. A typical four-mirror laser cavity [5] was designed in such a way that the size of the output laser mode was sensitive to the thermal lens in the crystal. The cavity consisted of a highly-reflective (HR, at 0.75 μm) plane mirror M1, two HR concave folding mirrors R1 and R2 (radius of curvature, Roc: 100 mm), and a plane output coupler (OC) with a transmission of 5 % at the laser wavelength. The mirror R1 which served as a pump mirror was coated for high transmission (HT) at 0.532 μm. The laser crystal was pumped by a CW green 2ω Nd:YVO_4 laser (Finesse, Laser Quantum) emitting up to 6 W at 0.532 μm (a diffraction-limited output, TEM_{00} mode). The pump was focused into the Alexandrite crystal by a 150 mm lens. At the focus the pump spot diameter $2w_p$ was ~25 μm in the vertical direction and ~44 μm in the horizontal one (due to the Brewster-angle oriented crystal). The crystal was pumped in a single-pass and about 85 % of the pump was absorbed.

For the measurements of the laser beam radius, a 150 mm spherical lens placed at 34.8 cm after the OC, a cut-off filter for the green (0.532 μm) and a beam profiler were used as shown in Fig. 1(b).

We started with characterization of the CW laser regime. The Alexandrite laser, Fig. 1(a), operated at 0.7509 μm (fractional quantum defect for the pump and laser photons, $\eta_q = 1 - \lambda_p/\lambda_L = 29.2$ %). The laser output was linearly polarized (***E*** ∥ ***b***). The maximum output power reached 1.11 W with a slope efficiency of 26.8 % (with respect to the absorbed pump power P_{abs}). The optical-to-optical efficiency with respect to the incident pump power (P_{inc}) was ~18%.

In Fig. 2, we show the spatial profiles of the output mode from the Alexandrite laser corresponding to various levels of output power. Close to the laser threshold, the beam profile was nearly circular. At higher pump powers, the beam was distorted and became elliptic with its major semi-axis

being parallel to the horizontal direction *x*. This indicated the action of an astigmatic thermal lens. To proceed with the ABCD modeling of thermal lens, the M^2 parameters of the laser beam were measured along the *x* and *y* directions using a standard ISO procedure (with a focusing lens, see Fig. 1(b)).

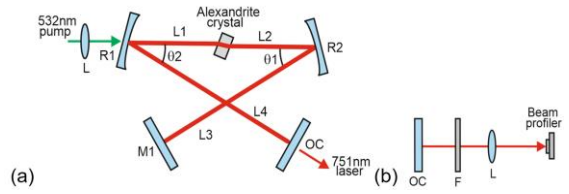

Fig. 1. (a) Schematic of the CW Alexandrite laser: M1 - HR plane mirror, R1 and R2 – HR concave folding mirrors (Roc = 100 mm), OC - output coupler, L1 = 53 mm, L2 = 48.5 mm, L3 = 802 mm, L4 = 702 mm, θ1 = θ2 = 9°; (b) set-up for the thermal lens measurement: F – filter, L – lens

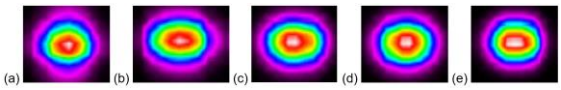

Fig. 2. Spatial profiles of the laser mode from the Alexandrite laser corresponding to the various output power levels: (a) 0.18 W; (b) 0.40 W; (c) 0.65 W; (d) 0.87 W; (e) 1.11 W. The laser polarization, **E** ∥ **b**, is horizontal, the **a**-axis is vertical

An example of evaluation of the beam quality factors, $M^2_{x,y}$, for the Alexandrite laser operating at maximum output power is shown in Fig. 3(a). The beam quality factors were $M^2_x = 1.85$ and $M^2_y = 1.47$. The measured $M^2_{x,y}$ parameters plotted *vs*. P_{abs} are presented in Fig. 3(b). The beam quality was lower (M^2 is higher) in the horizontal direction. With the increase of the pump power, both $M^2_{x,y}$ parameters tend to increase.

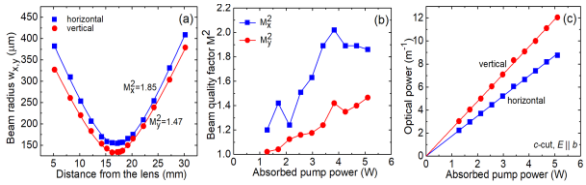

Fig. 3. (a) Evaluation of the beam quality factor M^2 for the Alexandrite laser (P_{abs} = 5.1 W) in horizontal and vertical directions, x and y, respectively; (b) measured $M^2_{x,y}$ parameters for the Alexandrite laser; (c) determined optical power of the thermal lens $D_{x,y}$: symbols – experimental data, lines – their linear fits for the calculation of the sensitivity factors $M_{x,y}$.

The results on the calculated optical power of the thermal lens $D_{x,y}$ are shown in Fig. 3(c). The thermal lens is positive for both directions (also referred as principal meridional planes). The optical power increases linearly with the absorbed pump power. This dependence is typically expressed by the so-called sensitivity factors, $M_{x,y} = dD_{x,y}/dP_{abs}$. In our case, $M_x = 1.74$ and $M_y = 2.38$ m^{-1}/W. The error in the determination of *M*-factors was 0.05 m^{-1}/W. The difference in the *M*-factors is expressed by the astigmatism degree, $S/M = |M_y - M_x|/M_y = 27\%$ ($S/M = 0\%$ for a spherical lens and 100% for a cylindrical one). Note that the difference of *M*-factors can be partially attributed to the different radii of the pump beam in the Brewster-angle oriented laser crystal. The radius of the pump beam is larger in the horizontal direction, so weaker thermo-optic aberrations are expected. However, one cannot describe the two directions separately, as the temperature field is formed in a bulk crystal.

For a longitudinally laser-pumped active element, the sensitivity factor of the thermal lens can be theoretically calculated as $M_{x,y} = \eta_h \Delta_{x,y}/(2S_p\kappa)$ [6], where $\eta_h \approx \eta_q$ is the fractional heat loading approximated as a quantum defect in the case of Alexandrite, $\Delta_{x,y}$ is the "generalized" thermo-optic coefficient (representing a joint action of the thermo-optic, photo-elastic and thermal expansion effects), $S_p = \pi \square w_p \square \square/\cos(\theta_B)$ is the effective pump spot area accounting for the Brewster-angle orientation of the laser crystal and the divergence of the pump beam, $\square w_p \square \square \sim 70$ μm is the root-mean square radius of the pump beam averaged through the whole length of the laser crystal. According to this formula, we estimated $\Delta_{x,y} = 2S_p\kappa M_{x,y}/\eta_h$, resulting in $\Delta_x = 10.1$ and $\Delta_y = 13.8 \times 10^{-6}$K^{-1} values.

To conclude, we experimentally studied measure the thermal lens in a laser alexandrite (Cr^{3+}:$BeAl_2O_4$) element using a green-laser-pumped ***c***-cut Alexandrite crystal emitting at 0.7509 μm with the ***E*** ∥ ***b*** polarization. The sensitivity factors of the thermal lens under highly focused pump were as weak as $M_x = 1.74$ and $M_y = 2.38$ m^{-1}/W and the astigmatism degree for a Brewster-oriented laser element was only 27%. The optical power of the thermal lens was varying linearly with the absorbed pump power. Positive thermal lens in Alexandrite makes it suitable for microchip-type lasers.

We believe that a detailed knowledge of the thermal lensing properties of Alexandrite crystal will help in designing laser cavities of high-power CW and ML oscillators based on the Kerr lensing, SESAMs, graphene or their combination [7, 8].

References

1. J.C. Walling, O.G. Peterson, H.P. Jenssen, R.C. Morris, and E. W. O'Dell, "Tunable Alexandrite lasers,"IEEE J. Quantum Electron. 16(12), 1302–1315 (1980).

2. J. Walling, F.H. Donald, H. Samelson, D.J. Harter, J. Pete, and R.C. Morris, "Tunable Alexandrite lasers: development and performance," IEEE J. Quantum Electron. 21(10), 1568–1581 (1985).

3. C.F. Cline, R.C. Morris, M. Dutoit, and P.J. Harget, "Physical properties of BeAl2O4 single crystals," J. Mater. Sci. 14(4), 941–944 (1979).

4. S.R. Scheps, B.M. Gately, J.F. Myers, J.S. Krasinski, and D.F. Heller, "Alexandrite laser pumped by semiconductor lasers," Appl. Phys. Lett. 56(23), 2288–2290 (1990).

5. S. Ghanbari and A. Major, "High power continuous-wave Alexandrite laser with green pump," Laser Phys. 26(7), 075001 (2016).

6. S. Chenais, F. Druon, S. Forget, F. Balembois, and P. Georges, “On thermal effects in solid-state lasers: The case of ytterbium-doped materials,” Prog. Quantum Electron. 30(4), 89–153 (2006).

7. R. Akbari, K.A. Fedorova, E.U. Rafailov, and A. Major, “Diode-pumped ultrafast Yb:KGW laser with 56 fs pulses and multi-100 kW peak power based on SESAM and Kerr-lens mode locking,” Appl. Phys. B 123(4), 123 (2017).

8. C. Cihan, C. Kocabas, U. Demirbas, and A. Sennaroglu, “Graphene mode-locked femtosecond Alexandrite laser,” Opt. Lett. 43(16), 3969–3972 (2018).

УДК 535.37

ОПРЕДЕЛЕНИЕ ПАРАМЕТРОВ КРОСС-РЕЛАКСАЦИИ В ОКСИФТОРИДНЫХ ТУЛИЕВЫХ СТЕКЛАХ

Ясюкевич А.С.[1], Демеш М.П.[1], Гусакова Н.В.[1], Кулешов Н.В.[1], Рачковская Г.Е.[2], Захаревич Г.Б.[2]

[1]НИЦ Оптических материалов и технологий БНТУ
Минск, Республика Беларусь
[2]Белорусский государственный технологический институт,
Минск, Республика Беларусь

Тулиевые материалы – кристаллы и стекла, активированные ионами трехвалентного тулия (Tm^{3+}) – широко используются как активные среды для создания лазерных источников света в практически важной области спектра 1.8–2 мкм.

Накачка таких лазеров часто осуществляется по следующей схеме: возбуждение ионов тулия на уровень $^3H_4$ излучением диодных лазеров на длине волны ≈800 нм; перенос энергии возбуждения на верхний лазерный уровень $^3F_4$. Эффективным механизмом такой передачи энергии является кросс релаксация по схеме:

$$^3H_6+{}^3H_4\rightarrow{}^3F_4+{}^3F_4$$

при этом квантовая эффективность накачки приближается к 2.

Схема нижних уровней Tm^{3+} с указанием основных переходов представлена на рис. 1

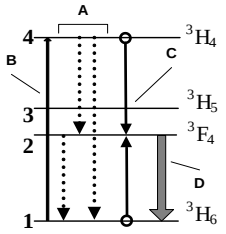

Рисунок 1. – Нижние уровни иона Tm^{3+} и основные переходы:
А – внутрицентровая релаксация; *В* – возбуждение, *С* – кросс-релаксация; *Д* – генерация

Исследование кинетики затухания люминесценции с уровня $^3H_4$ (например, переход $^3H_4\rightarrow{}^3F_4$) позволяет установить доминирующий характер Д-А взаимодействия и определить концентрационную зависимость параметров, определяющих эффективность переноса энергии в тулиевых средах за счет кросс-релаксационного механизма. Здесь, донор (Д) – ион тулия на уровне $^3H_4$, акцептор (А) – ион тулия на уровне $^3H_6$.

В качестве объекта исследования в данной работе выбраны образцы оксифторидных стекол с ионами тулия следующего состава:

$$30\ SiO_2+10\ GeO_2+X\ PbO+(50\text{-}X)\ PbF_2+$$
$$+10\ CdF_2+Y\ Tm_2O_3,$$

здесь X=5 (образцы А), 25 (образцы В), 45 (образцы С). Для каждого из образцов А, В и С величина Y=0.01, 0.1, 0.5 и 1.

Следуя методике, использованной в [1], было установлено, что для ионов тулия в стеклах, изучаемых в данной работе, доминирующим является квадруполь-квадрупольное Д-А взаимодействие, и было оценено время внутрицентровой релаксации τ_4 уровня $^3H_4$, которое составляет ≈ 300 мкс.

Значение τ_4 было использовано при аппроксимации кривых затухания люминесценции на переходе $^3H_4\rightarrow{}^3F_4$ формулой, предложенной в [2]:

$$I(t)=I(t=0)\exp\left(-t/\tau_4-\gamma_S t^{3/S}\right). \qquad (1)$$

Коэффициент γ_S отвечает за статический неупорядоченный перенос энергии от Д к А, S=10 (квадруполь-квадрупольный механизм переноса энергии). γ_S напрямую связан с микропараметром C_{DA}, который определяет вероятность прямой передачи энергиии при парном взаимодействии Д и А.

$$C_{DA}=\frac{\gamma_S^{S/3}}{\left[\frac{4}{3}\pi N_{Tm}\Gamma\left(1-\frac{3}{S}\right)\right]^{S/3}}, \qquad (2)$$

где Γ – гамма-функция. В литературе параметр C_{DA} часто используют, для оценки вероятности переноса энергии в коллективе доноров и акцепторов. Можно показать, что для такого случая вероятность дезактивации уровня $^3H_4$ за счет кросс-релаксации W_{CR} можно оценить по формуле:

$$W_{CR}=C_{DA}\left(\frac{4\pi}{3}\right)^{S/3}N_{Tm}^{S/3} \qquad (3)$$

и при S=10

$$W_{CR}=0.419\gamma^{10/3} \qquad (4)$$

Величину W_{CR} также можно найти непосредственно из системы скоростных уравнений,